Reliability Evaluation of Bulk Power System Considering Compressed Air Energy Storage

Osama Aslam Ansari, *Student Member, IEEE*, Safal Bhattarai, *Student Member, IEEE,* Rajesh Karki, *Senior Member*, *IEEE*, C. Y. Chung, *Fellow, IEEE*

***Abstract*—The integration of large-scale energy storage systems (ESSs) have been identified as a viable option to mitigate the adverse effects of renewable energy sources (RES) on the power system operation and reliability. Currently, compressed air energy storage (CAES) is one of the two large-scale energy storage technologies with low capital and operational costs. This paper presents a method to integrate a new CAES reliability model in the bulk power system reliability evaluation and investigates quantitative benefits derived from the CAES. A state-duration sampling method is adopted for the reliability evaluation. A detailed reliability model of the CAES that considers its actual operating mechanism is first developed. Each system contingency state is then analyzed using a unit commitment (UC) method instead of hourly optimal power flow (OPF). This ensures that the inter-temporal constraints introduced by the CAES, such as its state-of-charge (SOC), are included in the analysis. Case studies are performed on a six-bus test system containing a wind farm and a CAES. The results indicate that the CAES can improve the overall reliability of the system. In particular, the reliability indices of the bus where the CAES is connected show the greatest improvement.**

***Index Terms*— Compressed air energy storage, reliability evaluation, bulk system, Monte-Carlo, Latin Hypercube Sampling, reliability**

I. NOMENCLATURE

The terminologies used in this paper are listed as follows:

Sets/Indices

i	Index of bus
l	Index of line
κ	Index of scenario
t	Index of hour
Ω_{G}	Set of conventional generators
Ω_{B}	Set of all buses
Ω_C	Set of buses with a CAES

Parameters

c_i^{vom}	Variable operation and maintenance cost ($/MWh)
ru_i	Ramp-up rate limit of generator at bus i (MW/h)
rd_i	Ramp-down rate limit of generator at bus i (MW/h)
$d_i^{\kappa,t}$	Electricity load demand at bus i (MW)
$f_l^{\kappa,\max}$, $f_n^{\kappa,\max}$	The maximum power flow of lines l and n, respectively (MW)
$\overline{g}_i^{\kappa}$, $\underline{g}_i^{\kappa}$	Maximum, minimum power output of generator at bus i (MW)
$\rho_{j,\mathrm{su/sd}}^{\mathrm{G}}$	Start-up/shut-down cost for conventional generator j
$\overline{p}_{i,\mathrm{ch/dch}}^{\kappa}$	Maximum charging/discharging power
$\underline{p}_{i,\mathrm{ch/dch}}^{\kappa}$	Minimum charging/discharging power
T_κ	Total number of hours in each contingency scenario
$M_{i,l}$	The element in the ith row and the lth column of node-branch incidence matrix
$\overline{W}_i^{\kappa}$	Maximum wind power that can be generated at bus i (MW)
$\tilde{\gamma}_l$	Susceptance of a line l (Siemens)
ρ_i^g	Generation cost of generator i ($/MWh)
ρ_i^L	Penalty cost for electricity load loss at bus i ($/MWh)
ρ_i^s	Penalty cost for wind spillage at bus i ($/MWh)
Δt	Time duration (1 hour)

Variables

f_l^{κ}	Total active power flow on line l (MW)
g_i^{κ}	Power output of generator at bus i (MW)
$p_{i,\mathrm{ch}}^{\kappa,t}$	Charging power of CAES at bus i (MW)
$p_{i,\mathrm{dch}}^{\kappa,t}$	Discharging power of CAES at bus i (MW)
r_i^{κ}	Electricity load loss at bus i (MW)
$I_{i,t}^{\kappa}$	Binary variable indicating online/offline status of the generator i : 1 if it is online, 0 otherwise
S_i^{κ}	Wind power curtailment at bus i (MW)
$W_i^{\kappa,t}$	Scheduled wind power generation at bus i (MW)
$\alpha_i^{\kappa,t}$	Binary variable indicating start-up of generator i
$\beta_i^{\kappa,t}$	Binary variable indicating shut-down of generator i
$\alpha_{i,\mathrm{ch}}^{\kappa,t}$	Binary variable indicating charging status of CAES at bus i : 1 if it is charging, 0 otherwise
$\alpha_{i,\mathrm{dch}}^{\kappa,t}$	Binary variable indicating discharging status of CAES at bus i : 1 if it is discharging, 0 otherwise
$\theta_{l,\mathrm{fr/to}}^{\kappa}$	Phase angle of from/to-side node of line l (rad)

II. INTRODUCTION

OWING to the adverse effects of conventional sources of electricity generation on the environment, the penetration of renewable energy sources (RES), such as solar and wind power, in the existing power system is gradually increasing throughout the world. In this regard, renewable portfolio standards (RPS) have been widely accepted in many different

This work is supported by the Natural Sciences and Engineering Research Council (NSERC) of Canada.

The authors are with the Department of Electrical and Computer Engineering, University of Saskatchewan, Saskatoon, SK, Canada (e-mail: oa.ansari@usask.ca, safal.bhattarai@usask.ca, rajesh.karki@usask.ca, c.y.chung@usask.ca)

978-1-5386-0817-3/17/$31.00 ©2017 IEEE

countries [1]. These standards bound the electric utilities to produce a certain percentage of their total generation from RES. From the electric utilities' point of view, the integration of RES brings many new challenges to the reliable planning and operation of a power system. RES are inherently intermittent and stochastic in nature and hence high penetration of such sources can cause large imbalances between the load and generation. Furthermore, in certain situations, the power system may not be able to utilize the available output from RES due to congestion. In these cases, the output of RES has to be curtailed. To mitigate these negative impacts of RES, energy storage systems (ESSs) have become indispensable components of a power system containing a large proportion of renewable energy generation. ESSs can help in managing the peak demand, load leveling, reducing line congestion and gaining financial advantage from energy arbitrage [2]. Also, ESSs can provide grid related ancillary services such as voltage regulation, power quality and black start [2], [3]. Various ESSs technologies include compressed air energy storage (CAES), pumped hydro storage (PHS), flywheel, battery ESSs (BESSs) etc. [3]. CAES is a large-scale storage technology with relatively low capital and operational costs. The CAES uses electrical energy to convert ambient air into high pressure compressed air and stores it into a reservoir which is usually an underground cavern [3]. The compressed air is then utilized to produce electricity when required.

ESSs require large initial investment for their construction. The inclusion of ESSs in the existing power system can be justified if certain benefits in terms of reduction in operational costs, and improvement in system reliability are obtained from them. The impacts of ESSs on the overall system reliability and economy have been studied from various perspectives. The reliability evaluation of a small isolated wind energy conversion system (WECS) with BESSs has been performed in [4]. Reference [5] presents a Monte-Carlo simulation based technique to assess the reliability benefits of ESSs considering different operating strategies and wind energy dispatch restrictions. The analysis is carried out for the generation system, that is, at HL-1. In [6], a reliability assessment method based on the combination of analytical and simulation based approaches has been proposed for a WECS with BESS. The BESS is connected to the doubly fed induction generator (DFIG)-based wind turbine at the DC-link of the power converter. In [7], the operational strategies for ESSs are proposed to improve the reliability of a distribution system with load aggregation. In [8], a method based on sequential Monte-Carlo simulation (SMCS) is proposed to evaluate the reliability and economy of distribution system containing ESSs. The method considers the optimal operation of distribution system's load aggregator and islanding feature of the system. Reference [9] considers the ramp up and ramp down capabilities of conventional generators and ESSs in the evaluation of the operational reliability of the system. In [10], the ESSs operated by the wind farm operator is utilized to decrease the operating risk of the power system.

The previous work presented in the literature utilizes a generic reliability model of the ESSs. However, different ESSs may have entirely different operating mechanisms. Hence, it is important to take into account the actual operation scheme which is specific for a certain type of ESSs. Therefore, in this paper, a reliability model of the CAES is developed. The model takes into account different failure events that may occur during the operation of the CAES. Afterward, the reliability model is included in the simulation-based method to evaluate the reliability of a bulk power system (HL-II). In the simulation-based evaluation methods, based on the failure and repair rates of components, a large number of contingency states are generated. Then in each contingency state, optimal power flow (OPF) is used to reschedule the generation to minimize the load curtailment. However, the single-hour OPF cannot consider the coupling between different hours. This link which is introduced by the SOC of the CAES can be taken into account by considering the daily unit commitment (UC). Hence, in this paper for the system analysis, 24-hour UC is utilized to reschedule the generation, CAES and other resources to minimize the load curtailment.

The rest of the paper is organized as follows. Section III presents the reliability model of the CAES. Section IV describes the simulation method for reliability evaluation. In Section V, the optimization problem for system analysis is presented. Section VI presents the overall reliability evaluation method. Case studies are performed in Section VII. Section VIII provides the conclusion of the work.

III. Reliability Modelling of CAES

In order to accurately determine the reliability impacts of the CAES, it is important to consider the actual operation of such a system. The block diagram of a conventional CAES is shown in Fig. 1. The principle of operation of a CAES is similar to the operation of a conventional gas turbine. The only difference is that, in CAES, the compression and expansion cycles are separated in two different stages. During charging, the air at ambient conditions is compressed using multi-stage compressors and is stored inside the cavern at high pressure. During discharging, the air from the cavern is released, combusted and expanded in the turbines. An accurate reliability model of CAES should consider the interaction between different parts of the system and the possible failure events of different components in the system. For the reliability modeling of a conventional gas turbine, the two-state continuous-time Markov model has been widely used that represents the complete system either in upstate or in downstate as illustrated in Fig. 2 [11]. A similar two-state model can be used in case of the CAES with appropriate values of transition rates between the two states. However, this two-state model does not accurately represent the operation of the CAES.

Since the charging and discharging parts of the CAES are separated, the failures of the components in the charging part will not affect the operation of discharging part and vice versa. To represent this behavior, a four-state model is developed as shown in Fig 3. In this model, the charging and discharging processes are decoupled. The up-state (state 1) represents the situation when all the components of the CAES are available. State 2 corresponds to the failure in the charging part. State 3 relates to the failure in the discharging part. State 0 represents

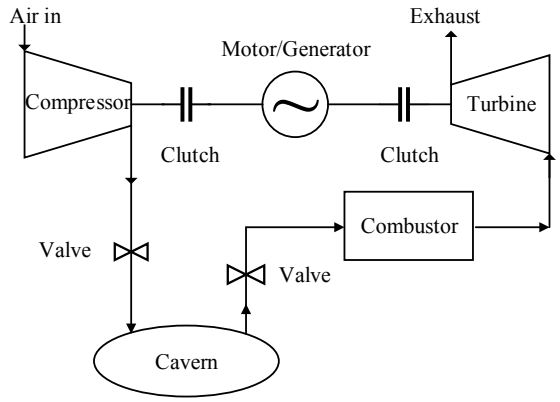

Fig. 1. CAES system diagram

the complete failure state. This state occurs when either both charging and discharging parts are failed or when the motor/generator set is failed. Hence, the CAES can neither be used for charging or discharging.

The different transition rates among the states represent the possible failure events. In the subsequent studies, it is assumed that during one time period, only one transition can occur. Hence, the transition rates between states 2 and 3 are assumed to be zero. Also, it is assumed that once the CAES is in down state (state 0), the CAES is brought to the up state after the complete repair process. And, therefore, the transition rates from state 0 to states 2 and 3 are assumed to be zero. In the following sections, this model for the CAES is utilized for the reliability studies.

IV. Simulation Methodology

In power system reliability studies, SMCS is widely employed to simulate the system and obtain the reliability indices [12], [13]. The main advantages of the SMCS are that this simulation is independent of the size of the system and that the chronology of the events is maintained. This chronology is important when CAES is included in the system. This is because of the fact that the SOC of the CAES links different hours in the simulation period. Hence, the chronology of the events will affect the operation of the CAES. A major drawback of SMCS is that it requires a large number of iterations before it converges. In this regard, different variance reduction techniques such as Latin Hypercube Sampling (LHS), importance sampling and dagger sampling etc. have been utilized to speed up the rate of convergence of the simulation [12]. In this paper, LHS is employed for the simulation. Unlike Monte-Carlo (MC) simulation which utilizes random numbers to generate the samples from a probability distribution, LHS stratifies the probability distribution so that the samples are obtained from equally spaced intervals of the distribution. This ensures that those events which are less probable but have high impact are also included in the samples. In this work, state-duration method is adopted for the simulation. In this method, the component state duration distribution functions are used to generate the chronological component state transition process. Afterward, the system's chronological state transition process is created from the combination of components' processes [12].

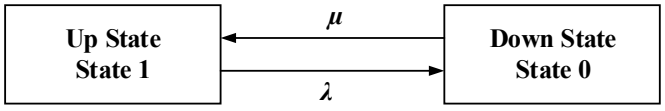

Fig. 2. Two state model

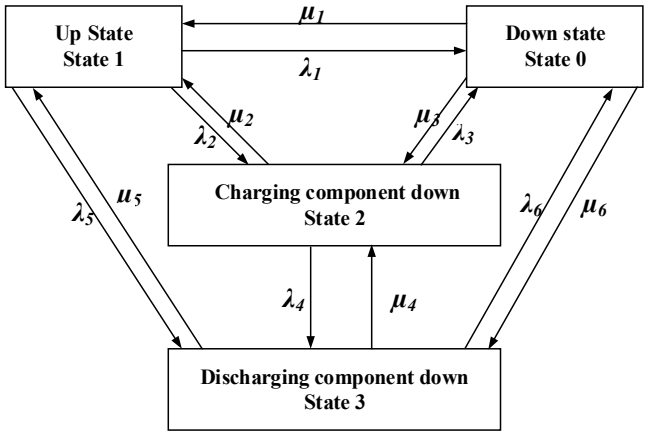

Fig. 3. Four state model of CAES

V. System Analysis

In power system reliability studies, after generating different contingencies states, single-hour OPF is utilized to reschedule the generation as a result of contingencies [12]. The objective is to minimize load curtailment. However, as mentioned earlier this method is not suitable in the presence of the CAES. The reason being is that the different hours of operation of the system are coupled through the SOC of the CAES. Therefore, in this work, a daily UC is used to reschedule the generation in the presence of contingencies. After simulating a large number of contingency states of the system, these states for 24 hours are aggregated to form contingency scenarios and then the daily UC optimization problem is solved.

The optimization problem for a daily UC is given by (1) – (20).

$$\text{Min.} \quad \sum_{t=1}^{T}\sum_{j\in\Omega_{\mathrm{G}}}\left(\rho_{j,\mathrm{su}}\alpha_{j,\kappa,t}^{\mathrm{G}}+\rho_{j,\mathrm{sd}}\beta_{j,\kappa,t}^{\mathrm{G}}\right)+\sum_{i\in\Omega_B}\left(\sum_{t=1}^{T_\kappa}\left(\rho_j^{\mathrm{G}}g_i^{\kappa,t}\Delta t+\rho_i^{\mathrm{W}}S_i^{\kappa,t}\Delta t+\rho_i^{\mathrm{L}}r_i^{\kappa,t}\Delta t+c_i^{\mathrm{vom}}\left(p_{i,\mathrm{ch}}^{\kappa,t}+p_{i,\mathrm{dch}}^{\kappa,t}\right)\Delta t\right)/T_\kappa\right) \quad (1)$$

s.t.

$$\sum_{l\in\Omega}M_{i,l}\,f_l^{\kappa,t}+g_i^{\kappa,t}+W_i^{\kappa,t}+r_i^{\kappa,t}-d_i^{\kappa,t}+p_{i,\mathrm{dch}}^{\kappa,t}-p_{i,\mathrm{ch}}^{\kappa,t}=0,\ \forall i\in\Omega_B,\forall t\in\Omega_T,\forall\kappa \quad , \quad (2)$$

$$f_l^{\kappa,t}-\tilde{\gamma}_l\left(\theta_{l,\mathrm{fr}}^{\kappa,t}-\theta_{l,\mathrm{to}}^{\kappa,t}\right)=0,\forall l\in\Omega,\forall t\in\Omega_T,\forall\kappa \quad , \quad (3)$$

$$\left|f_l^{\kappa,t}\right|\le f_l^{\kappa,\max},\ \forall l\in\Omega_{\mathrm{L}},\ \forall t\in\Omega_T,\forall\kappa \quad , \quad (4)$$

$$I_{i,t}^{\kappa}\underline{g}_i^{\kappa}\le g_{i,t}^{\kappa}\le I_{i,t}^{\kappa}\overline{g}_i^{\kappa},\ \forall i\in\Omega_B,\ \forall t\in\Omega_T,\forall\kappa \quad , \quad (5)$$

$$g_{i,t+1}^{\kappa}-g_{i,t}^{\kappa}\le ru_i,\ \forall i\in\Omega_B,\ \forall t\in\Omega_T,\forall\kappa \quad , \quad (6)$$

$$g_{i,t}^{\kappa}-g_{i,t+1}^{\kappa}\le rd_i,\ \forall i\in\Omega_B,\ \forall t\in\Omega_T,\forall\kappa \quad , \quad (7)$$

$$\alpha_{i,t}^{\mathrm{G},\kappa}-\beta_{i,t}^{\mathrm{G},\kappa}=I_{i,t}^{\kappa}-I_{i,t-1}^{\kappa},\ \forall i\in\Omega_B,\ \forall t\in\Omega_T,\forall\kappa \quad , \quad (8)$$

$$\sum_{t}^{t+T_{i,\min}^{\mathrm{on}}-1}I_{i,t}^{\kappa}\ge\alpha_{i,t}^{\kappa}T_{i,\min}^{\mathrm{on}},\ \forall i\in\Omega_B,\ \forall t\in\left\{1,\dots,T_\kappa-T_{i,\min}^{\mathrm{on}}+1\right\},\forall\kappa \quad , \quad (9)$$

$$\sum_{t}^{T_\kappa}I_{i,t}^{\kappa}\ge\alpha_{i,t}^{\kappa}(T_\kappa-t+1),\ \forall i\in\Omega_B,\ \forall t\in\left\{T_\kappa-T_{i,\min}^{\mathrm{on}}+2,\dots,T_\kappa\right\},\forall\kappa \quad , \quad (10)$$

$$\sum_{t}^{t+T_{i,\min}^{\mathrm{off}}-1}\left(1-I_{i,t}^{\kappa}\right)\ge\beta_{i,t}^{\kappa}T_{i,\min}^{\mathrm{off}},\ \forall i\in\Omega_B,\ \forall t\in\left\{1,\dots,T_\kappa-T_{i,\min}^{\mathrm{off}}+1\right\},\forall\kappa \quad , \quad (11)$$

$$\sum_{t}^{T_\kappa}\left(1-I_{i,t}^{\kappa}\right)\ge\beta_{i,t}^{\kappa}(T_\kappa-t+1),$$

$$\forall i \in \Omega_B,\ \forall t\ \left\{T_\kappa - T^{\text{off}}_{i,\min} + 2, \dots, T_\kappa\right\}, \forall \kappa \quad , \quad (12)$$

$$S_i^{\kappa,t} + W_i^{\kappa,t} = \overline{W}_i^{\kappa,t},\ \forall i \in \Omega_B,\ \forall t \in \Omega_T, \forall \kappa \quad , \quad (13)$$

$$0 \le W_i^{\kappa,t},\ \forall i \in \Omega_B,\ \forall t \in \Omega_T, \forall \kappa \quad , \quad (14)$$

$$0 \le S_i^{\kappa,t},\ \forall i \in \Omega_B,\ \forall t \in \Omega_T, \forall \kappa \quad , \quad (15)$$

$$r_i^{\kappa,t} \le d_i^{\kappa,t},\ \forall s \in \Omega_B,\ \forall t \in \Omega_T, \forall \kappa \quad , \quad (16)$$

$$\alpha_{i,\text{ch}}^{\kappa,t} + \alpha_{i,\text{dch}}^{\kappa,t} \le 1,\ \forall s \in \Omega_C,\ \forall t \in \Omega_T, \forall \kappa \quad , \quad (17)$$

$$E_s^{\kappa,t} = E_s^{\kappa,t-1} - \left(p_{i,\text{ch}}^{\kappa,t} - p_{i,\text{dch}}^{\kappa,t}\right)\Delta t\ , \quad \forall s \in \Omega_C,\ \forall t \in \Omega_T, \forall \kappa\ , \quad (18)$$

$$\alpha_{i,\text{ch}}^{\kappa,t}\underline{p}_{i,\text{ch}}^{\kappa} \le p_{i,\text{ch}}^{\kappa,t} \le \alpha_{i,\text{ch}}^{\kappa,t}\overline{p}_{i,\text{ch}}^{\kappa},\ \forall s \in \Omega_C,\ \forall t \in \Omega_T, \forall \kappa\ , \quad (19)$$

$$\alpha_{i,\text{dch}}^{\kappa,t}\underline{p}_{i,\text{dch}}^{\kappa} \le p_{i,\text{dch}}^{\kappa,t} \le \alpha_{i,\text{dch}}^{\kappa,t}\overline{p}_{i,\text{ch}}^{\kappa}, \quad \forall s \in \Omega_C,\ \forall t \in \Omega_T, \forall \kappa\ . \quad (20)$$

The objective function is given in (1). The objective function includes the start-up, shut-down and the running costs of the conventional generators, wind spillage costs, load shedding costs and operational costs of the CAES. The power balance and line flow constraints are given by (2) and (3) respectively. The limits on the line flows, and conventional generators' output are given by (4) and (5). Constraints (6) and (7) represent the ramp down and ramp up limits respectively. The constraints for minimum up and down times of the conventional generators are formulated by (8) – (12). Constraints (13) – (15) represent the limits on the wind spillage. The load curtailment is limited by (16). And the constraints for CAES and its SOC are represented by (17) – (20). This problem is solved for each contingency scenario.

VI. Reliability Evaluation Method

The complete methodology of the reliability evaluation is shown in Figure 4. In the first step, the up times and down times for all of the components in the system are generated using the method described in Section IV. These components include generators, transmission lines, and the CAES. For each of these components, except CAES, a two-state Markov model is used. For CAES, the four-state model developed in Section III is employed. These up times and down times are generated for a large number of sample years to ensure that all the possible combinations of up and down states of different components are sampled. The wind power is then simulated for the same duration. The wind power can be simulated either by sampling the probability distribution of the wind speed using inverse transformation and then converting it to wind power [13], or by generating the time-series from different time-series models [5]. The load can also be generated using the same method as that of wind power.

Afterward, the up and down times, as well as wind power and load, are divided into blocks of 24 hours. For each block of 24 hours, some of the components can be in the down state while other components can be in the up state. Then, for each 24-hours block, the optimization problem presented in Section V is solved. The solution determines the optimal generation output and CAES output (charging or discharging) for each hour of the 24-hours block. It also determines the total load that is curtailed during each of the 24-hours blocks due to components' failures. The load curtailment in each hour contributes to the system unreliability and hence take part in the evaluation of reliability indices. Subsequently, further blocks of 24-hours are analyzed until one year is completed. At the end of each year, the reliability indices are evaluated. The calculations are repeated for a large number of simulation years. Certain convergence criteria such as one based on the coefficient of variation can be employed for convergence of the simulation.

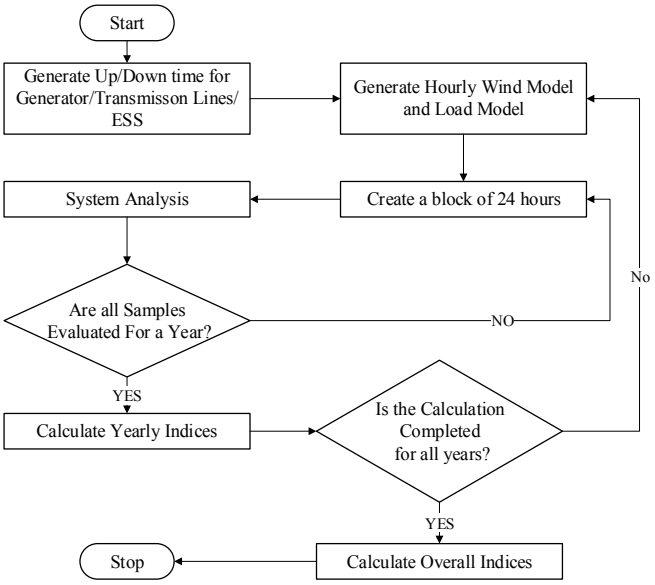

Fig. 4 Complete Methodology

VII. Case Studies And Results

A. Test System

The reliability evaluation method is applied to a six-bus test system shown in Fig. 5 [14]. The reliability data for the generators are obtained from [15], and are shown in Table I. For the transmission lines, the failure rate and repair rate are assumed to be 0.150 f/yr and 547.5 r/yr respectively [15]. The test system is modified by introducing one wind farm at bus 4 and one CAES at bus 5. The rating of the wind farm is set to 100 MW. The operational data related to CAES are shown in Table II. Table III provides the assumed transition rates for the four-state model of the CAES. All the other transition rates, except the ones provided in the table, are assumed to be zero. These values of transition rates are selected such that the

TABLE I
Test System Data

Generator	Maximum Power (MW)	Minimum Power (MW)	Operating Cost ($/MWh)	Start-up Cost ($)	Shut-down Cost ($)	Min. Up Time (h)	Min. Down Time (h)	Failure Rate (f/yr)	Repair Rate (r/yr)
1	220	100	13.51	300	50	4	4	4	196
2	100	10	32.63	200	0	2	3	2.4	157.6
3	20	10	17.70	250	30	1	1	3.0	147.0

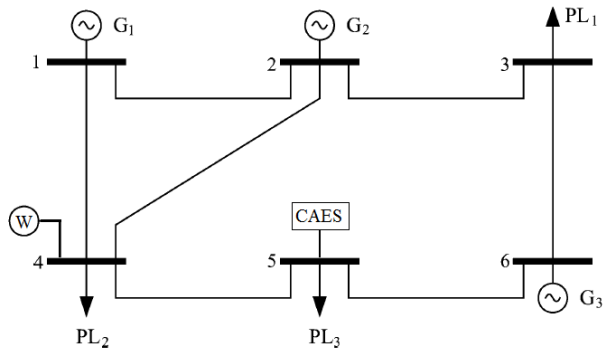

Fig. 5 6-Bus Test System

availability of the CAES matches the actual values [3]. The load model is obtained from RBTS whereas the wind profile is simulated using the time-series provided in [5]. The peak load of the system is 256 MW. The costs of load curtailment and wind spillage are set to \$1000/MWh and \$500/MWh respectively.

B. Reliability Indices

The reliability indices used in the current study include the probability of load curtailment (PLC), the expected energy not supplied (EENS), the expected demand not supplied (EDNS), the bulk power energy curtailment index (BPECI) and the severity index (SI). PLC measures the reliability of the system in terms of simple probability. EENS measures the expected amount of energy that the system is unable to supply due to random outages, EDNS describes EENS in terms of load demand, BPECI normalizes the EENS with respect to peak load so that different systems can be compared, SI, also known as system minutes, implies that if an outage happens during the occurrence of the peak load, how much time would that outage last for. These indices are evaluated at the system level as well as at individual load points. The detailed descriptions and formulations of all indices are given in [11].

C. Results

In order to quantify the benefits derived from the CAES in terms of system reliability and operational cost, the following two different cases are analyzed:

Case 1: Bulk power system without CAES

Case 2: Bulk power system with CAES

TABLE II
CAES DATA

Max. Discharging Power (MW)	Max. Charging Power (MW)	Energy Capacity (MWh)	Operational Cost (\$/MWh)
60	290	580	3.59

TABLE III
TRANSITION RATES

Failure Rates	f/yr	Repair Rates	r/yr
λ_1	5	μ_1	250
λ_2	4	μ_2	150
λ_3	5	μ_5	200
λ_5	4.5		
λ_6	5		

TABLE IV
SYSTEM INDICES

Case	PLC	EENS (MWh/yr)	EDNS (10^{-3} MW/yr)	BPECI (MWh/ MW-yr)	SI (syst-min)
Case 1	0.0415323	137.514	15.698	0.537164	32.2298
Case 2	0.0016597	5.440	0.621	0.021250	1.27505

TABLE V
LOAD POINT INDICES

Case	Load	PLC (10^{-3})	EENS (MWh/ yr)	EDNS (10^{-3} MW/yr)	BPECI (MWh /MW-yr)	SI (syst-min)
Case 1	PL_1	9.33557	19.434	2.218551	0.3795	22.77
	PL_2	35.9368	107.56	12.22791	1.0504	63.02
	PL_3	4.61055	10.514	1.200314	0.1026	6.169
Case 2	PL_1	0.33827	0.6511	0.07432	0.0127	0.762
	PL_2	1.46634	4.4089	0.50329	0.0430	2.581
	PL_3	0.15453	0.3801	0.04339	0.0037	0.220

The results for both cases are shown in Tables IV and V. System indices are shown in Table IV. Whereas Table V indicates the load point indices. It can be seen that CAES can bring significant benefit to the system in terms of reliability. There has been a marked decrease in the values of PLC, EENS, EDNS, BPECI and SI, from case 1 to case 2. Similarly, the load point indices' reliability is also improved. The load point PL_3 is at bus 5 where the CAES is connected. In case 2, it can be seen that this load point has the highest reliability among all the other load points. This is because the output of CAES can directly support the load point PL_3 in the case of contingencies and the output of CAES to that load point is not constrained by transmission line flows.

In order to understand the economic effect of the inclusion of CAES in the system, it is important to evaluate the yearly operating costs. Also, the total wind spillage in both cases can further justify the inclusion of CAES in the system. The yearly operating costs for case 1 and case 2 are \$ 19.561M/yr and \$ 16.265M/yr respectively. Most of the additional cost in case 1 is because of the load curtailment costs. Moreover, there is a decrease in the wind spillage from case 1 to case 2. The wind spillage in case 2 reduces by 87% as compared to that in case 1. This shows that the CAES is highly effective in integrating the

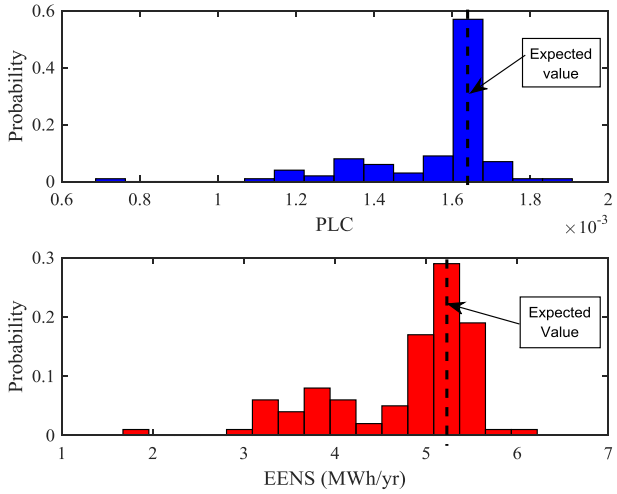

Fig. 6 Probability distribution of PLC and EENS

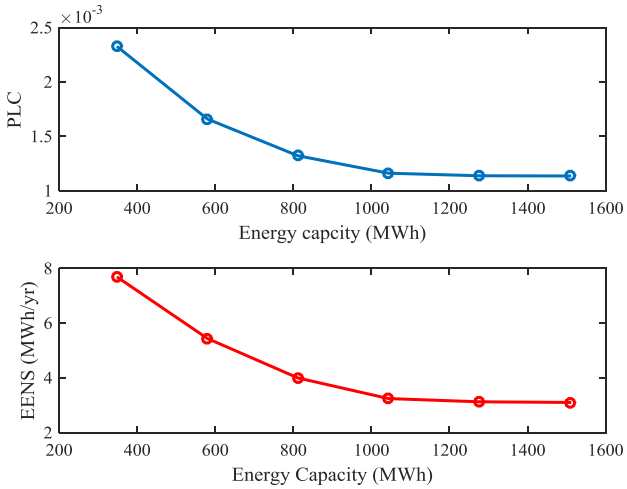

Fig. 7 Effect of energy capacity of CAES on reliability indices

wind power and thereby supporting the integration of renewable energy.

For case 2, the probability distributions of PLC and EENS are shown in Fig. 6. It can be observed that the distribution of PLC is mainly concentrated around the average value, whereas for EENS, it is fairly distributed.

D. Sensitivity Analysis

In order to understand the effect of CAES capacity on the reliability indices, sensitivity analysis is performed. The size of CAES is changed and the corresponding changes in the values of PLC and EENS are observed. The results are shown in Fig. 7, which indicates that the reliability of system increases as the energy capacity of CAES is increased. However, after a certain increase in the capacity, the reliability of the system does not improve but saturates to a constant value. In other words, the incremental increase in reliability decreases as the capacity of CAES increases. This is because of the inherent energy limitations of the wind generation. In order to further increase the reliability, additional wind farms may be installed, rather than installing a CAES with larger capacity.

To study the effect of the siting of CAES in the system, a sensitivity study is performed by changing the location of the CAES. Since there are six buses in the system, therefore there are six positions for siting CAES. The results are shown in Table VI. From the results, it can be observed that in terms of PLC and EENS, bus 4 is the most suitable location for constructing the CAES. Also, the load buses are more suitable than generation buses for constructing the CAES. This is again because of the fact that the output of CAES is not constrained by the transmission line limits if CAES is at the same bus as that of the load. The maximum difference in the values of PLC and EENS for different buses is 21.9% and 2.76% respectively.

TABLE VI
SENSITIVITY ANALYSIS

Bus No.	PLC	EENS (MWh/yr)	EDNS (10^{-3} MW/yr)	BPECI (MWh/ MW-yr)	SI (syst-min)
1	0.0021119	5.5080735	0.62877	0.02151	1.2909
2	0.0020650	5.5939675	0.63858	0.02185	1.3110
3	0.0016586	5.4683164	0.62423	0.02136	1.2816
4	0.0016529	5.4390326	0.62089	0.02124	1.2747
5	0.0016597	5.4402205	0.62102	0.02125	1.2750
6	0.0017090	5.4787719	0.62543	0.02140	1.2840

VIII. CONCLUSION

In this work, the reliability evaluation of a bulk power system (HL-II) considering wind power and compressed air energy storage system (CAES) is performed. The results indicated that the addition of CAES can bring significant benefits to the power system. It has been shown that CAES cannot only improve reliability but it can also increase the wind penetration in the system by reducing the wind spillage. It was observed that the bus where the CAES was connected showed the greatest improvement in reliability. Sensitivity studies were also performed to understand the effects of the sizing and siting of CAES on the reliability indices. Further studies can be performed to understand the effect of changing load curtailment and wind curtailment cost on the reliability metrics.

REFERENCES

[1] M. Jaccard, "Renewable Portfolio Standard," E.-C. C. J. Cleveland, Ed. New York; Elsevier, 2004, pp. 413-421.

[2] D. Manx, R. Piwko, and N. Miller, "Look before you leap: The role of energy storage in the grid," *IEEE Power and Energy Magazine*, vol. 10, no. 4, pp. 75-84, Jul.-Aug. 2012.

[3] X. Luo, J. Wang, M. Dooner, and J. Clarke, "Overview of current development in electrical energy storage technologies and the application potential in power system operation", *Applied Energy*, vol. 137, pp. 511-536, 2015.

[4] R. Billinton, Bagen, and Y. Cui, "Reliability evaluation of small stand-alone wind energy conversion systems using a time series simulation model," *IEE Proceedings- Generation, Transmission and Distribution*, vol. 150, no. 1, pp. 96-100, Apr. 2003.

[5] P. Hu, R. Karki and R. Billinton, "Reliability evaluation of generating systems containing wind power and energy storage" *IET Generation Transmission and Distribution*, vol. 3, no. 8, pp. 783-791, Aug. 2009.

[6] F. A. Bhuiyan, A. Yazdani, "Reliability assessment of a wind-power system with integrated energy storage," *IET Renewable Power Generation*, vol.3, no. 3, pp. 211-220, May 2010.

[7] Y. Xu and C. Singh, "Power system reliability impact of energy storage integration with intelligent operation strategy," *IEEE Trans. Smart Grid,* vol. 5, no. 2, Mar. 2014.

[8] Y. Xu and C. Singh, "Adequacy and economy analysis of distribution systems integrated with electric energy storage and renewable energy resources," *IEEE Trans. Power Syst.,,* vol. 27, no. 4, pp. 2332–2341, Nov. 2012

[9] P. Wang, Z. Gao, and L. Bertling. "Operational Adequacy Studies of Power Systems with Wind Farms and Energy Storages." *IEEE Trans. Power Syst.* vol. 27, no. 4, pp. 2377-2384, Nov. 2012.

[10] S. Thapa, and R. Karki, "Reliability benefit of energy storage in wind integrated power system operation," *IET Generation, Transmission & Distribution,* vol. 10, no. 3, pp. 807-814, Mar. 2016.

[11] R. Billinton and R. N. Allan, "*Reliability evaluation of power systems*". Springer, 1996.

[12] R. Billinton and W. Li, *Reliability Assessment of Electrical Power Systems Using Monte Carlo Methods*. New York: Plenum, 1994.

[13] O. A. Ansari, N. Safari, and C. Y. Chung, "Reliability assessment of microgrid with renewable generation and prioritized loads," *in 2016 IEEE Green Energy and Systems Conference (IGESC)*, Long Beach, 6-7 Nov. 2016.

[14] L. Wu, M. Shahidehpour, and T. Li, "Stochastic security-constrained unit commitment," *IEEE Trans. Power Syst.,* vol. 22, no. 2, pp. 800-811, May 2007.

[15] R. Billinton et.al, "A reliability test system for educational purposes – basic data", *IEEE Trans. Power Syst.,* vol. 4, no. 3, pp. 1238-1244, Aug. 1989.